Journal of Quantitative Spectroscopy & Radiative Transfer 138 (2014) 107–115

Contents lists available at ScienceDirect

Journal of Quantitative Spectroscopy & Radiative Transfer

journal homepage: www.elsevier.com/locate/jqsrt

Einstein *A*-values and oscillator strengths of the $A^2\Pi$–$X^2\Sigma^+$ system of CP

R.S. Ram [a], J.S.A. Brooke [a], C.M. Western [b], P.F. Bernath [a,c,*]

[a] Department of Chemistry, University of York, Heslington, York YO10 5DD, UK
[b] School of Chemistry, University of Bristol, Bristol BS8 1TS, UK
[c] Department of Chemistry and Biochemistry, Old Dominion University, Norfolk, VA 23529, USA

ARTICLE INFO

Article history:
Received 9 November 2013
Received in revised form
17 January 2014
Accepted 30 January 2014
Available online 8 February 2014

Keywords:
Line strengths
Einstein *A* coefficients
Oscillator strengths
Carbon stars

ABSTRACT

Line strengths for bands of the $A^2\Pi$–$X^2\Sigma^+$ transition of CP, including the effect of rotation on the vibrational wavefunctions (the Herman–Wallis effect), have been calculated using Western's PGOPHER program and Le Roy's LEVEL program. The potential energy functions for the $A^2\Pi$ and $X^2\Sigma^+$ state were computed using spectroscopic constants obtained from high resolution spectra. The RKR potentials of the two states, and the electronic transition dipole moments of this transition calculated in a recent *ab initio* study have been used in Le Roy's LEVEL program to produce transition dipole moment matrix elements. The matrix elements have been converted from Hund's case (b) to (a), and then used in PGOPHER to generate a line list containing observed and calculated wavenumbers, Einstein *A* coefficients and *f*-values for 75 bands with $v=0$–8 for both states. The Einstein *A* coefficients have been used to compute radiative lifetimes for $v=0$–5 in the $A^2\Pi$ state. The line list may be useful for computing the molecular opacities of CP needed to simulate the spectra of stellar and substellar sources.

1. Introduction

Among the phosphorus-containing diatomic radicals, CP, PN and PO have been found in circumstellar shells. The CP radical was first observed in the envelope of the obscured carbon star IRC+10216 by Guélin and coworkers [1] in 1990. They observed the $N=2\rightarrow1$, $3\rightarrow2$ and $5\rightarrow4$ lines with some partially resolved fine and hyperfine components. Since then, the millimeter-wave spectrum of IRC+10216 was surveyed with the IRAM 30-m telescope by Cernicharo et al. [2], and CP and PN were identified along with several other carbon-containing species. Recently, PN and PO have also been observed in the shell of the oxygen-rich red supergiant, VY CMa, by Ziurys et al. [3] and Tenenbaum et al. [4]. More recently, Milan and coworkers [5] have re-measured the $N=5\rightarrow4$ transition towards IRC+10216 during an investigation of phosphorus chemistry in carbon- and oxygen-rich circumstellar envelopes, and an abundance of the order of $\sim1\times10^{-8}$ has been obtained for CP relative to molecular hydrogen.

CP is isovalent to the CN and SiN free radicals. The first spectroscopic identification of CP was made by Herzberg [6] in 1930 through the observation of the $B^2\Sigma^+$–$X^2\Sigma^+$ transition, which is analogous to the violet system of CN. A rotational analysis of this transition was performed by Baerwald et al. [7], who also reported the $B^2\Sigma^+$–$A^2\Pi$ transition in the visible region. The rotational structure of the $B^2\Sigma^+$–$A^2\Pi$ transition was investigated by Chaudhry and Upadhya [8], and later by Tripathi et al. [9] using spectra recorded with grating spectrometers.

The first observation of the $A^2\Pi$–$X^2\Sigma^+$ transition of CP, which is analogous to the red-system of CN, was reported in the near infrared by Ram and Bernath [10]. CP was produced using a microwave discharge source by the

* Corresponding author. Tel.: +1 757 683 3807.
E-mail address: pbernath@odu.edu (P.F. Bernath).

http://dx.doi.org/10.1016/j.jqsrt.2014.01.030
0022-4073

reaction of carbon deposited on the inner walls of the discharge tube with a slow flow of phosphorus vapor. Improved spectroscopic constants for the ground and excited electronic states were provided from the rotational analysis of five vibrational bands of the $A^2\Pi$–$X^2\Sigma^+$ transition. In another study, the millimeter-wave transitions of CP in its ground state were measured by Saito et al. [11] and precise spectroscopic constants were obtained. Pure rotational terahertz spectra were also measured by Klein et al. [12]. In another study [13], several more bands of the $A^2\Pi$–$X^2\Sigma^+$ transition were analyzed, and improved spectroscopic constants for the v', $v''=0$–4 vibrational levels were obtained in fits that included hyperfine-corrected pure rotational transition frequencies [11].

In some early theoretical studies of CP, potential energy curves, Franck–Condon factors and *r*-centroids have been calculated [14–17]. In a very recent study, Shi et al. [18] have employed the MRCI method (including spin-orbit coupling) to calculate the potential energy curves and spectroscopic properties of the ground state and many excited electronic states. Rohlfing and Almlöf [19] used large scale MRCI calculations employing atomic natural orbital basic sets to calculate the dipole moment, vibrational frequency and bond length in the ground state. de Brouckère and Feller [20] have also calculated various properties of the ground state and provided predictions of several pure rotational transitions in the $v=0$–9 vibrational levels. In another theoretical study Gu et al. [21] have performed an *ab initio* study of a number of electronic states, including the Einstein *A* coefficients and oscillator strengths of some low-lying doublet and quartet transitions, and predicted radiative lifetimes for the $A^2\Pi$, $B^2\Sigma^+$ and $1^4\Pi$ states. Chandler et al. [22] have performed SCF calculations on the ground states and selected excited states of a number of molecules including CN, CP and SiN. de Brouckère [23] has performed configuration interaction calculations on the $X^2\Sigma^+$ state and de Brouckère and Feller [24] have performed similar calculations on the $A^2\Pi_i$ state and the $A^2\Pi$–$X^2\Sigma^+$ transition of CP to calculate many properties, including the electronic transition dipole moment (TDM) function of the $A^2\Pi$–$X^2\Sigma^+$ transition.

In the present paper we report on the calculation of line intensities in the form of Einstein *A* coefficients and oscillator strengths (*f*-values) for the $A^2\Pi$–$X^2\Sigma^+$ transition of CP using Le Roy's LEVEL [25] program and Western's PGOPHER [26] program, and the calculated TDM function of de Brouckère and Feller [24]. We have included the effect of rotation on the vibronic transition dipole moment. A line list has been generated, which consists of observed and calculated wavenumbers, Einstein *A* values and oscillator strengths (*f*-values) for rotational lines up to $J=60.5$, in 75 bands with vibrational levels with $v=0$–8 in the ground and excited states. These data may prove useful in astronomical studies of CP in carbon stars and other cool sources.

2. Treatment of experimental data

In the previous studies of CP [10,13], the rotationally-resolved line positions of the $A^2\Pi$–$X^2\Sigma^+$ transition were measured from the spectra recorded using the Fourier transform spectrometer of the National Solar Observatory at Kitt Peak. In these studies, the spectroscopic constants were determined using a least-squares fitting program in which the observed vibration–rotation lines [10,13] and the hyperfine-free pure rotational transitions generated from the microwave measurements of CP by Saito et al. [11] were fitted simultaneously. The same input data has now been refitted using PGOPHER with the addition of the terahertz lines of Klein et al. [12] (not included earlier). We made slight adjustments in the higher order constants of the $v'=3$ and 4 levels. For example, the constant A_D of $v'=3$ has been fixed at 2.00×10^{-5} cm^{-1} based on the A_D values of 4.869×10^{-5}, 4.305×10^{-5}, 3.038×10^{-5} cm^{-1}, respectively, for the $v'=0$, 1 and 2 levels. Also, the constant p_D of $v'=3$ was not well determined from the free fit, and therefore it was fixed at -0.88×10^{-7} cm^{-1}, the value determined for the $v=2$ level. Since only the $^2\Pi_{3/2}$–$^2\Sigma^+$ sub-band for $v'=4$ ($^2\Pi_{3/2}$–$^2\Sigma^+$, 4–3 band) was observed in the previous study [13], the constants *A*, A_D, *q*, and p_D were fixed at values close to the values for the $v'=3$ level. As expected, the fit is very similar but with a slight change in some higher order constants, and an improvement in the constants for $v''=0$. The spectroscopic constants of the $X^2\Sigma^+$ and $A^2\Pi$ states obtained from the PGOPHER fit are provided in Tables 1 and 2, respectively. These constants were used to obtain equilibrium constants for the two states, which are provided in Table 3. In this work we have computed the intensity of the bands with $v=0$–8 for both states. Therefore, we have estimated the values of the

Table 1
Spectroscopic constants[a] (in cm^{-1}) for the $X^2\Sigma^+$ state of CP.

v	T_v	B_v	$D_v\times10^6$	$\gamma_v\times10^2$
0	0	0.7958810907(66)	1.328045(11)	1.8566387(96)
1	1226.12738(28)	0.78989476(80)	1.33152(43)	1.85056(75)
2	2438.57460(27)	0.78389278(88)	1.33625(54)	1.84458(80)
3	3637.33389(35)	0.7778735(13)	1.34164(96)	1.8390(10)
4	4822.3972(14)	0.771835(11)	1.345(20)	1.8376(73)
5	5993.7542[b]	0.7657875[b]	1.360[b]	1.8215[b]
6	7151.3992[b]	0.7597194[b]	1.371[b]	1.8036[b]
7	8295.3229[b]	0.7536349[b]	1.383[b]	1.7770[b]
8	9425.5171[b]	0.7475339[b]	1.396[b]	1.7395[b]

[a] Values in parentheses are one standard deviation in the last two digits.
[b] Values fixed by extrapolation.

Table 2
Spectroscopic constants[a] (in cm^{-1}) for the $A^2\Pi$ state of CP.

v	T_v	A_v	$A_{D_v} \times 10^5$	B_v	$D_v \times 10^6$	$q_v \times 10^5$	$p_v \times 10^3$	$P_{D_v} \times 10^7$
0	6884.00566(21)	−156.24385(22)	4.869(25)	0.70927602(56)	1.28042(29)	−4.791(64)	9.410(18)	−1.26(15)
1	7934.41445(22)	−156.12665(31)	4.305(43)	0.70364906(66)	1.28296(37)	−4.85(13)	9.436(25)	−1.06(22)
2	8972.76570(26)	−156.04334(37)	3.038(62)	0.69801455(94)	1.28510(66)	−4.89(12)	9.632(39)	−0.88(48)
3	9999.06544(36)	−156.01825(22)	2.00[c]	0.6923799(13)	1.29156(89)	−4.96(16)	10.161(20)	−0.88[c]
4	11013.30165(66)	−156.02[c]	2.00[c]	0.6867172(27)	1.2928(21)	−4.96[c]	14.9(17)	−0.88[c]
5	12015.5285[b]	−156.02[c]	2.00[c]	0.68107774[b]	1.29[c]	−4.96[c]	14.9[c]	−0.88[c]
6	13005.7038[b]	−156.02[c]	2.00[c]	0.67541868[b]	1.29[c]	−4.96[c]	14.9[c]	−0.88[c]
7	13983.8485[b]	−156.02[c]	2.00[c]	0.66975316[b]	1.29[c]	−4.96[c]	14.9[c]	−0.88[c]
8	14949.9680[b]	−156.02[c]	2.00[c]	0.66408118[b]	1.29[c]	−4.96[c]	14.9[c]	−0.88[c]

[a] Values in parentheses are one standard deviation in the last two digits.
[b] Values fixed by extrapolation.
[c] Fixed close to the value for the last vibrational level varied.

Table 3
Equilibrium constants (in cm^{-1}) for the $X^2\Sigma^+$ and $A^2\Pi$ states of CP.

Constants	$X^2\Sigma^+$	$A^2\Pi$
T_e	0.0	6972.46893(53)
ω_e	1239.79987(11)	1062.4724(14)
$\omega_e x_e$	6.834102(48)	6.03353(88)
$\omega_e y_e \times 10^2$	−0.13211(62)	0.105(15)
B_e	0.79886750(33)	0.7120860(26)
$\alpha_e \times 10^2$	0.596862(74)	0.56184(34)
$\gamma_e \times 10^5$	−0.856(17)	−0.403(85)
R_e (Å)	1.56197826(32)	1.6544214(30)

spectroscopic constants for the unobserved $v=5$–8 levels using the equilibrium constants. The extrapolated constants of the $v=5$–8 levels are also provided in Tables 1 and 2.

3. Calculation of line intensities

As has been described in the previous studies of CaH [27], C_2 [28] and CN [29], the line intensities in an electronic transition of a diatomic molecule can normally be calculated in the form of Einstein A-coefficients using the following equation:

$$A_{J'\rightarrow J''} = 3.13618932 \times 10^{-7} \tilde{\nu}^3 \frac{S^{\Delta J}_{J''}}{(2J'+1)} |\langle \psi_{\nu'J'} | \mathscr{R}_e(r) | \psi_{\nu''J''} \rangle|^2 \quad (1)$$

in which the Einstein A values are in s^{-1}, $S^{\Delta J}_{J''}$ is the rotational line strength factor, also called the Hönl–London factor, $\tilde{\nu}$ is the transition wavenumber in cm^{-1}, $\mathscr{R}_e$ is the electronic TDM function in debye and ψ_{vJ} is the vibrational wavefunction for a vJ level (J appears in general because the centrifugal potential V_{cent} depends on J). $\mathscr{R}_e(r)$ can be calculated using the following equation:

$$\mathscr{R}_e(r) = \langle \psi'_{el}(r) | \boldsymbol{\mu}(r) | \psi''_{el}(r) \rangle \quad (2)$$

where $\psi_{el}(r)$ is an electronic wavefunction and $\boldsymbol{\mu}(r)$ is the electric dipole moment operator. The eigenvalues E_{vJ} and eigenfunctions $\psi_{vJ}(r)$ for a diatomic molecule with an effective potential $V_{eff}=V(r)+V_{cent}$ [30] can be determined by solving the one-dimensional radial Schrödinger equation. The potential energy function, $V(r)$, can, for example, be determined by the RKR (Rydberg–Klein–Rees) method using the spectroscopic constants in the program RKR1 written by Le Roy [31], or by *ab initio* calculations. The calculation of line intensities is greatly simplified using the program LEVEL [30], which uses the RKR potentials [31] of the two electronic states as input.

In the case of CP, the potential energy functions for the $X^2\Sigma^+$ and $A^2\Pi$ states were calculated using the equilibrium spectroscopic constants provided in Ref. [13]. Next, the calculated classical turning points of the two potentials were employed in LEVEL in addition to the electronic TDM function, $\mathscr{R}_e(r)$, calculated by de Brouckère and Feller [24]. LEVEL then calculates the wavefunctions, ψ_{vJ}, and provides the TDM matrix elements for different bands. The current version of LEVEL is limited only to singlet–singlet transitions, and therefore it cannot calculate Hönl–London factors for a $^2\Pi$–$^2\Sigma^+$ transition directly. TDM matrix elements are therefore calculated by LEVEL for a $^1\Pi$–$^1\Sigma^+$ transition, ignoring electron spin. The subsequent calculations using PGOPHER [25] allow the spin to be taken into account.

The separation into $S^{\Delta J}_{J''}$ and $|\langle \psi_{\nu'J'} | \mathscr{R}_e(r) | \psi_{\nu''J''} \rangle|$ in Eq. 1 is not possible here due to the way in which we account for the J dependence of the vibronic TDM (Section 3.2). Instead, PGOPHER calculates Einstein A-coefficients using the following equation [30]:

$$A_{J'\rightarrow J''} = 3.13618932 \times 10^{-7} \tilde{\nu}^3 \frac{S_{J'J''}}{(2J'+1)}, \quad (3)$$

where the line strength used here, $S_{J'J''}$, is the TDM (in debye squared) summed over the degenerate M components of the both states and the possible polarizations of the light:

$$S_{J'J''} = \sum_{p,M',M''} |\langle \psi_{\nu'J'M'} | \boldsymbol{\mu_p} | \psi_{\nu''J''M''} \rangle|^2. \quad (4)$$

3.1. Conversion of matrix elements from Hund's case (b) to (a)

As LEVEL does not include electron spin, the matrix elements are essentially Hund's case (b) matrix elements. The CP $A^2\Pi$ state however is case (a) and PGOPHER uses a case (a) basis set, and therefore the matrix elements from LEVEL need to be converted into case (a) matrix elements.

This transformation has been performed using the following equation:

$$\langle \eta'\Lambda'|T_q^k(J'\Omega'J\Omega)|\eta\Lambda\rangle = (-1)^{J'-\Omega'}\begin{pmatrix} J' & k & J \\ -\Omega' & q & \Omega \end{pmatrix}^{-1} \times \sum_{N,N'}(-1)^{N-N'+S+J+k+\Lambda}(2N+1)(2N'+1) \times \begin{pmatrix} J' & S & N' \\ \Omega' & -\Sigma & -\Lambda' \end{pmatrix}\begin{pmatrix} J & S & N \\ \Omega & -\Sigma & -\Lambda \end{pmatrix} \times \begin{Bmatrix} N' & J' & S \\ J & N & k \end{Bmatrix}\begin{pmatrix} N' & k & N \\ -\Lambda' & q & \Lambda \end{pmatrix}\langle \eta'\Lambda'|T_q^k(N'N)|\eta\Lambda\rangle \quad (5)$$

where $\langle \eta'\Lambda'|T_q^k(J'\Omega'J\Omega)|\eta\Lambda\rangle$ is the Hund's case (a) vibronic transition matrix element, which is here allowed to depend on J and Ω of the electronic states involved to allow for the Herman–Wallis effect (see Section 3.2). Similarly, $\langle \eta'\Lambda'|T_q^k(N'N)|\eta\Lambda\rangle$ is the corresponding Hund's case (b) matrix element. We performed this transformation previously in our calculations on the CN molecule [29], which included the equivalent $A^2\Pi$–$X^2\Sigma^+$ system, and that paper and its supplementary material should be referred to for full details of the transformation.

The sum in the above equation is over all N values that can contribute to a given J, normally two for each value of J. For a particular combination of J and J' only two distinct matrix elements are required as there is a symmetry relationship between two matrix elements where all the angular momentum projection quantum numbers have opposite signs.

The change in the matrix elements due to this procedure is usually quite small. Fig. 1 shows examples of the difference between intensities that have been calculated using the transformation, and without using it. It can be seen in the upper section of Fig. 1 that including the Herman–Wallis effect (as explained in the next section) without using this transformation will change the intensities of the Q branch incorrectly.

3.2. The Herman–Wallis Effect

The vibrational wavefunctions are affected by rotation due to the centrifugal potential [30], which in turn affects the TDM matrix elements. This is called the Herman–Wallis effect [30,32,33], and is caused primarily by the rotation of the molecule. Please note that the term "Herman–Wallis" traditionally refers to vibration–rotation transitions only and not electronic transitions, but the cause of the observed effect is the same, and so the term "Herman–Wallis" has been used for simplicity throughout this paper.

We have described our method of accounting for the Herman–Wallis effect for a $^2\Pi$–$^2\Sigma$ transition previously in our work on CN [29], and it will be briefly described here. A correction factor, the Herman–Wallis factor $F_{TDM}(m_{J'\Omega'J\Omega})$ is applied to the TDM matrix element, where $m_{J'\Omega'J\Omega}$ is J'' for $\Delta J=-1$, $J''-0.5$ for $\Delta J=0$, and $J''+1$ for $\Delta J=+1$ (these values of $m_{J'\Omega'J\Omega}$ were used to obtain the best fit), and

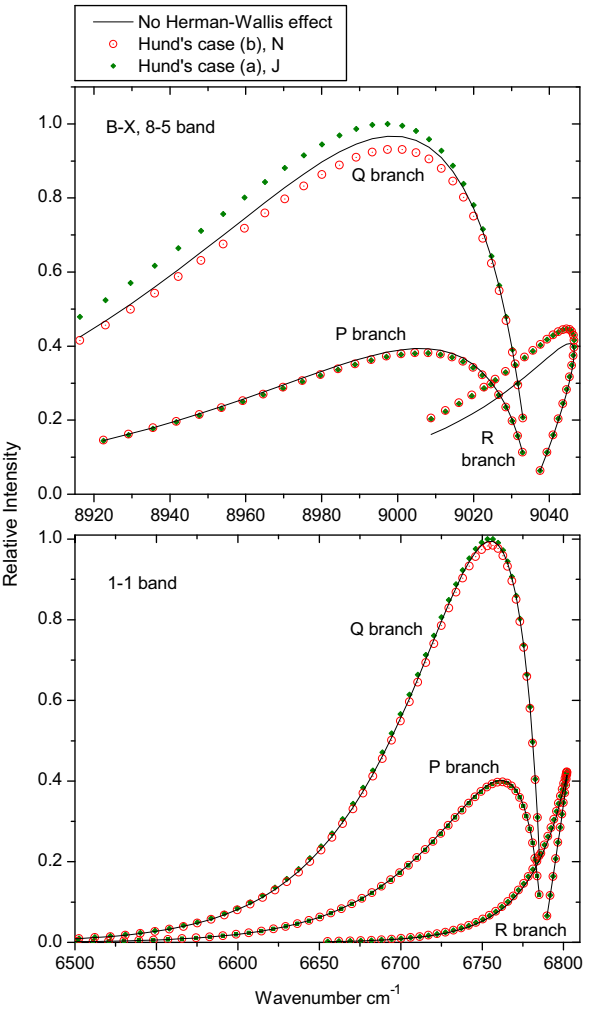

Fig. 1. Relative intensities of the CP $A^2\Pi$–$X^2\Sigma^+$, 1–1 and 8–5 bands. The black lines are calculated by using only one TDM matrix element for the whole band and including no Herman–Wallis effect. The green diamonds include the Herman–Wallis effect and the Hund's case (b) to (a) transformation of the matrix elements as described in the paper. The red circles are calculated by not performing Hund's case transformation, and using the quantum number N instead of J to account for the Herman–Wallis effect. For both parts of the figure, the intensities have been calculated using a rotational temperature of 500 K. J up to 55.5 is shown for the 1–1 band and to 30.5 for the 8–5 band. The 1–1 band was used as a typical example of the difference between the methods for the observed vibrational levels. The 8–5 band is shown as an example of when the Herman–Wallis effect is strong. (For interpretation of the references to color in this figure legend, the reader is referred to the web version of this article.)

where

$$F_{TDM}(m_{J'\Omega'J\Omega}) = \frac{\langle \eta'\Lambda'|T_q^k(J'\Omega'J\Omega)|\eta\Lambda\rangle}{\langle \eta'\Lambda'|T_q^k(J'=\Omega'\Omega'J=\Omega\Omega)|\eta\Lambda\rangle} \quad (6)$$

This can be expressed as a polynomial of the form

$$F_{TDM}(m_{J'\Omega'J\Omega}) = 1 + Cm_{J'\Omega'J\Omega} + Dm_{J'\Omega'J\Omega}{}^2 + Em_{J'\Omega'J\Omega}{}^3 + \ldots \quad (7)$$

Please note that this is not the standard definition of the Herman–Wallis factor, $F(m)$, and that $F(m) \approx F_{TDM}(m_{J'\Omega'J\Omega})^2$.

Normally, the TDM matrix elements in Eq. (6) would be squared and the correction factor would be applied to the overall line strength and not the TDM matrix elements (this is the reason for the "TDM" subscripts). This change has been made to make it possible to incorporate the Herman–Wallis effect into PGOPHER.

For each band, TDM matrix elements were calculated by LEVEL up to the maximum J level reported in the line list, and values of $F_{TDM}(m_{J'\Omega'J\Omega})$ obtained from Eq. (6). The Herman–Wallis parameters C, D, E etc. were derived by fitting the TDM matrix elements to $F_{TDM}(m_{J'\Omega'J\Omega})$ values, using Eq. (7) and with the polynomial orders adjusted to give a good fit. For each band six sets of parameters were derived, two for each of the P, Q and R branches, one for each upper level spin component. PGOPHER then takes these polynomial parameters and the values of Hund's case (a) matrix elements, $\langle \eta'\Lambda'|T_q^k(J'\Omega'J\Omega)|\eta\Lambda\rangle$ (one of these for each spin component and so two for each band). The Herman–Wallis coefficients used are available in online Supplement 1.

The Herman–Wallis effect in CP is small in the lower vibrational bands, but not negligible in the higher vibrational bands for which lines are reported. For example, the largest difference between the matrix elements for reported transitions within a vibrational band and the reference matrix element for that band (the denominator in Eq. 6) is 1.7% for the 0–0 band, 2.0% for the 4–3 band (the largest difference for an observed band), but 23% for the 5–3 band (the largest difference for any band), and so it was decided that it should be accounted for in the calculated linelist.

Table 4
Lifetimes (in μs) of the $A^2\Pi$ state of CP.

v	Present values		Gu et al. [21]
	$A^2\Pi_{1/2}$	$A^2\Pi_{3/2}$	
0	42.77	46.25	30.6
1	34.94	37.40	26.5
2	29.73	31.62	23.6
3	26.02	27.54	21.4
4	23.25	24.52	19.7
5	21.13	22.22	–

3.3. Line strengths and lifetimes

PGOPHER then calculates the Einstein A coefficients using Eq. (3) by combining the wavefunction coefficients from the diagonalization of the Hamiltonian in a Hund's case (a) basis with the vibronic transition dipole moments calculated as above. These are also converted into f-values (oscillator strengths) using the following equation:

$$f_{J'\rightarrow J''} = 1.49919368\,\frac{1}{\tilde{\nu}^2}\,\frac{(2J'+1)}{(2J''+1)}A_{J'\rightarrow J''}, \tag{8}$$

The radiative lifetimes for the $v=0$–5 vibrational levels of the $A^2\Pi_{1/2}$ and $A^2\Pi_{3/2}$ components were calculated using the Einstein A coefficients obtained from PGOPHER. In the calculation of the lifetime of a vibrational level of the $A^2\Pi_{1/2}$ component, the reciprocal of the sum of the Einstein A values of all possible transitions originating from $J=0.5$ of that vibrational level were calculated to provide the vibrational lifetime for that level. A similar calculation for all the transitions with $J'=1.5$ in the $A^2\Pi_{3/2}$ spin component provided the vibrational lifetimes for the $A^2\Pi_{3/2}$ component. So far no experimental values of lifetimes of electronic states of CP are available for comparison with our computed lifetimes. However, there is a theoretical study of lifetimes of the $A^2\Pi$, $B^2\Sigma^+$ and $1^4\Pi$ states of CP by Gu et al. [21]. Our computed values have been compared to the values of Gu et al. [21] in Table 4.

The lifetimes as a function of J were also calculated, and the relative change for each upper vibrational level is shown in Fig. 2. This change in lifetime with J is observed due to the inclusion of the Herman–Wallis effect in our calculations.

We have also calculated the vibrational Einstein $A_{v'v''}$ values and oscillator strengths ($f_{v'v''}$ values) for the bands of the $A^2\Pi$–$X^2\Sigma^+$ transition. In this calculation, $A_{v'v''}$ values for each band were calculated by taking the sum of all single rotational Einstein A values for possible transitions within the relevant band from the $J'=1.5$ level of the $A^2\Pi_{3/2}$ spin component and $J'=0.5$ of the $A^2\Pi_{1/2}$ spin component. We have found that the $A_{v'v''}$ values for the $A^2\Pi_{1/2}$–$X^2\Sigma^+$ and $A^2\Pi_{3/2}$–$X^2\Sigma^+$ sub-bands are slightly different. The Einstein $A_{v'v''}$ values for individual bands have been used to calculate the oscillator strength ($f_{v'v''}$) of

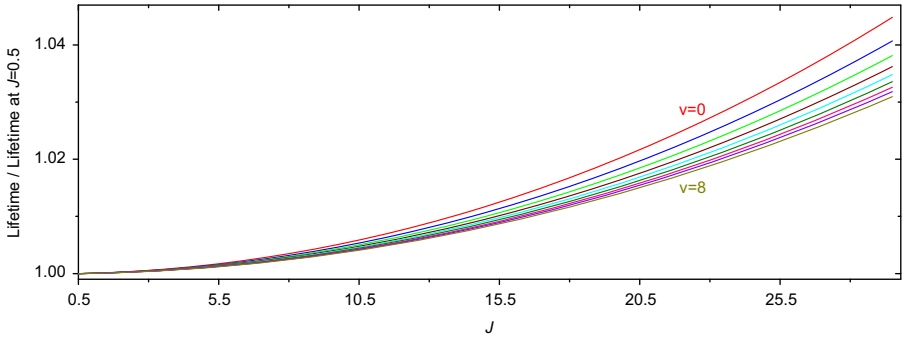

Fig. 2. Relative change in lifetimes with J for the $A^2\Pi$ state of CP, for vibrational levels up to $v=8$, and J up to 29.5. The relative change is shown as this makes it easier to compare the extent of the effect of J on the different vibrational levels. J is only shown up to 29.5 as higher J transitions were not calculated for many of the higher vibrational bands. Only the first and last vibrational bands are labeled as the plot lines are all in vibrational band order.

Table 5
Einstein $A_{v'v''}$ values[a] (in s^{-1}) for the $A^2\Pi$–$X^2\Sigma^+$ system of CP.

0	1	2	3	4	5	6	7	8
1.1996E+4	2.1952E+4	2.1754E+4	1.5621E+4	9.1584E+3	4.6740E+3	2.1568E+3	9.2176E+2	3.7173E+2
1.1205E+4	2.0692E+4	2.0648E+4	1.4906E+4	8.7772E+3	4.4954E+3	2.0805E+3	8.9141E+2	3.6027E+2
8.7226E+3	7.5678E+2	4.1607E+3	1.6027E+4	2.1748E+4	1.9148E+4	1.3147E+4	7.6760E+3	3.9950E+3
8.0287E+3	7.0574E+2	3.9165E+3	1.5193E+4	2.0732E+4	1.8334E+4	1.2635E+4	7.3993E+3	3.8610E+3
2.3618E+3	2.7088E+3	5.3041E+3	1.5159E+2	4.6827E+3	1.5852E+4	2.2007E+4	2.0454E+4	1.4988E+4
2.1253E+3	2.4873E+3	4.9372E+3	1.4251E+2	4.4336E+3	1.5096E+4	2.1053E+4	1.9641E+4	1.4437E+4
2.8729E+2	2.5952E+3	7.0080E+1	4.8586E+3	3.3164E+3	6.9997E+1	6.6227E+3	1.7193E+4	2.2538E+4
2.4865E+2	2.3271E+3	6.4182E+1	4.5138E+3	3.1124E+3	6.6178E+1	6.2996E+3	1.6432E+4	2.1624E+4
1.4302E+1	5.6968E+2	1.6084E+3	4.9481E+2	2.0648E+3	5.3160E+3	1.4034E+3	9.6327E+2	9.2563E+3
1.1391E+1	4.9004E+2	1.4367E+3	4.5202E+2	1.9143E+3	4.9809E+3	1.3254E+3	9.1520E+2	8.8378E+3
1.5944E-1	4.0141E+1	6.7175E+2	6.0568E+2	1.4527E+3	2.5814E+2	4.4501E+3	4.1173E+3	1.9047E+2
9.4030E-2	3.1527E+1	5.7401E+2	5.3884E+2	1.3233E+3	2.3881E+2	4.1625E+3	3.8830E+3	1.8080E+2
–	4.9125E-1	6.5219E+1	5.9373E+2	8.6282E+1	1.7460E+3	9.3815E+1	2.3061E+3	5.2974E+3
–	2.6950E-1	5.0425E+1	5.0368E+2	7.6425E+1	1.5857E+3	8.6612E+1	2.1532E+3	4.9887E+3
–	–	8.3351E-1	8.0075E+1	4.2316E+2	1.1379E+1	1.3733E+3	7.7952E+2	5.9603E+2
–	–	4.1625E-1	6.0822E+1	3.5617E+2	1.0034E+1	1.2433E+3	7.1793E+2	5.5549E+2
–	–	–	1.0237E+0	8.1848E+1	2.4569E+2	1.5397E+2	7.6220E+2	1.4281E+3
–	–	–	4.5019E-1	6.0930E+1	2.0504E+2	1.3509E+2	6.8778E+2	1.3120E+3

[a] Values in the upper and lower rows are the $A_{v'v''}$ values of the $A^2\Pi_{1/2}$–$X^2\Sigma^+$ and $A^2\Pi_{3/2}$–$X^2\Sigma^+$ sub-bands, respectively.

Table 6
Einstein $f_{v'v''}$ values[a] for the $A^2\Pi$–$X^2\Sigma^+$ system of CP.

0	1	2	3	4	5	6	7	8
7.4207E-4	1.0253E-3	7.9630E-4	4.6127E-4	2.2323E-4	9.5826E-5	3.7778E-5	1.3978E-5	4.9355E-6
7.2489E-4	1.0047E-3	7.8214E-4	4.5391E-4	2.2000E-4	9.4553E-5	3.7315E-5	1.3818E-5	4.8828E-6
7.9495E-4	4.9272E-5	2.0377E-4	6.1344E-4	6.7007E-4	4.8614E-4	2.8037E-4	1.3970E-4	6.2885E-5
7.7264E-4	4.8106E-5	1.9958E-4	6.0229E-4	6.5914E-4	4.7895E-4	2.7657E-4	1.3795E-4	6.2153E-5
3.4609E-4	2.6144E-4	3.6377E-4	7.7905E-6	1.8754E-4	5.0991E-4	5.8233E-4	4.5396E-4	2.8356E-4
3.3378E-4	2.5389E-4	3.5492E-4	7.6276E-6	1.8405E-4	5.0142E-4	5.7353E-4	4.4769E-4	2.7994E-4
7.7932E-5	4.0654E-4	7.1706E-6	3.5130E-4	1.7897E-4	2.9352E-6	2.2254E-4	4.7441E-4	5.2087E-4
7.4161E-5	3.9160E-4	6.9569E-6	3.4254E-4	1.7512E-4	2.8788E-6	2.1875E-4	4.6709E-4	5.1351E-4
9.3669E-6	1.6786E-4	2.6974E-4	5.3735E-5	1.5754E-4	3.0150E-4	6.1660E-5	3.3835E-5	2.6648E-4
8.6629E-6	1.5940E-4	2.5949E-4	5.2094E-5	1.5350E-4	2.9484E-4	6.0463E-5	3.3244E-5	2.6228E-4
5.0990E-7	2.9537E-5	2.1554E-4	1.0893E-4	1.6764E-4	2.0803E-5	2.6545E-4	1.8966E-4	6.9977E-6
4.2525E-7	2.7186E-5	2.0422E-4	1.0464E-4	1.6236E-4	2.0254E-5	2.5943E-4	1.8589E-4	6.8744E-6
–	1.9870E-6	5.4211E-5	2.0800E-4	1.6667E-5	2.1435E-4	7.9935E-6	1.4480E-4	2.5603E-4
–	1.6164E-6	4.9628E-5	1.9658E-4	1.5987E-5	2.0738E-4	7.7779E-6	1.4143E-4	2.5082E-4
–	–	4.3801E-6	7.5639E-5	1.6231E-4	2.3652E-6	1.7960E-4	7.0292E-5	3.9428E-5
–	–	3.4495E-6	6.8825E-5	1.5299E-4	2.2655E-6	1.7358E-4	6.8337E-5	3.8486E-5
–	–	–	7.2323E-6	8.8452E-5	1.0350E-4	3.4499E-5	1.0632E-4	1.3643E-4
–	–	–	5.4514E-6	7.9931E-5	9.7271E-5	3.2987E-5	1.0264E-4	1.3252E-4

[a] Values in the upper and lower rows are the $f_{v'v''}$ values of the $A^2\Pi_{1/2}$–$X^2\Sigma^+$ and $A^2\Pi_{3/2}$–$X^2\Sigma^+$ sub-bands, respectively.

these bands using the following equation:

$$f_{v'\to v''} = 1.49919368\frac{1}{\tilde{\nu}^2}\frac{(2-\delta_{0,\Lambda'})}{(2-\delta_{0,\Lambda''})}A_{v'\to v''} \quad (9)$$

where Kronecker $\delta_{0,\Lambda}=1$ for a $^2\Sigma^+$ state and 0 for a $^2\Pi$ state and $\tilde{\nu}^2$ is the average band wavenumber (for this we have used the wavenumber of the $^qQ_2(0.5)$ line for the $A^2\Pi_{1/2}$–$X^2\Sigma^+$ sub-band and the $^rR_1(0.5)$ line for the $A^2\Pi_{3/2}$–$X^2\Sigma^+$ sub-

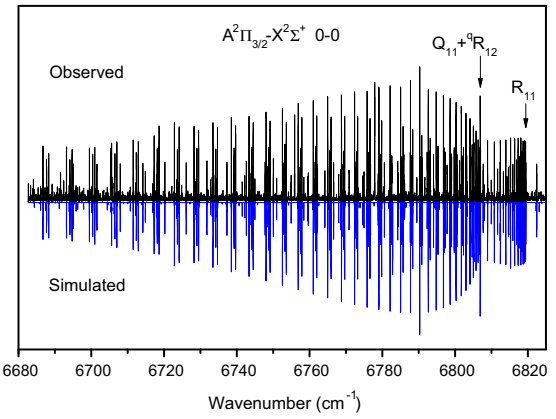

Fig. 3. A comparison of intensity distribution in the observed (upper) and simulated (lower) spectra of the $A^2\Pi_{3/2}$–$X^2\Sigma^+$, 0–0 band of CP, showing good agreement.

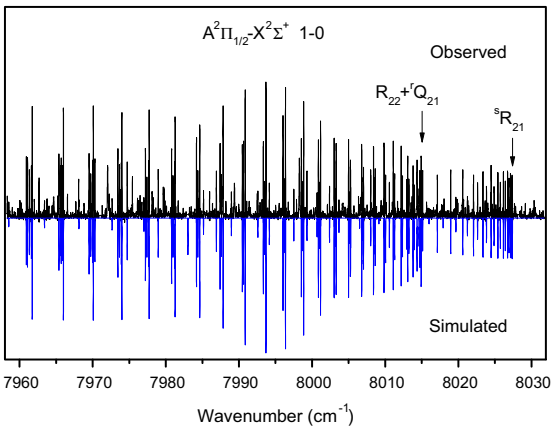

Fig. 4. A comparison of a portion of the observed (upper) and simulated (lower) spectra of the $A^2\Pi_{1/2}$–$X^2\Sigma^+$, 1–0 band of CP, showing a good correspondence between the two spectra.

band). Our computed values of the Einstein coefficients $A_{v'v''}$ and oscillator strengths $f_{v'v''}$ for the bands with $v=0$–8 are provided in Tables 5 and 6. Gu et al. [21] have also computed the Einstein coefficients $A_{v'v''}$ and oscillator strengths $f_{v'v''}$ for some low-lying transitions of CP. Our Einstein A values are lower than those calculated by Gu et al. [21] but their relative variation from band to band is very similar.

The $A^2\Pi$ state of CP is inverted and the $A^2\Pi_{1/2}$ component is about 156 cm^{-1} higher than the $A^2\Pi_{3/2}$ component. Eq. (1) shows that $A_{J'\to J''}$ is proportional to $\tilde{\nu}^3$ and $A_{J'\to J''}$ values of the two spin components are approximately related by the following equation:

$$A_{J'\to J''}(^2\Pi_{3/2}) = \left(\frac{\tilde{\nu}_{^2\Pi_{1/2}}}{\tilde{\nu}_{^2\Pi_{3/2}}}\right)^{-3} A_{J'\to J''}(^2\Pi_{1/2}) \qquad (10)$$

The $A_{00}=11205\ s^{-1}$, $A_{01}=8029\ s^{-1}$, $A_{02}=2125\ s^{-1}$ and $A_{03}=249\ s^{-1}$ values of the $A^2\Pi_{3/2}$ component (Table 5) convert to $A_{00}=11983\ s^{-1}$, $A_{01}=8712\ s^{-1}$, $A_{02}=2358\ s^{-1}$ and $A_{03}=287\ s^{-1}$ for the $A^2\Pi_{1/2}$ component using Eq. (10). These values are very similar to the respective derived values of $A_{00}=11996\ s^{-1}$ $A_{01}=8723\ s^{-1}$, $A_{02}=2362\ s^{-1}$, $A_{03}=287\ s^{-1}$ of the $A^2\Pi_{1/2}$ component. Our computed lifetimes of the two spin components are significantly longer than the lifetimes calculated by Gu et al. [21].

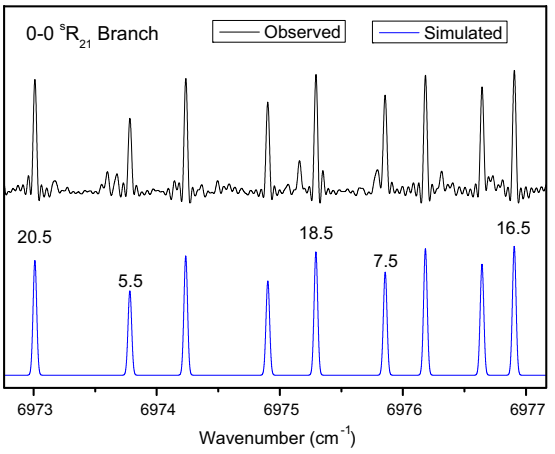

Fig. 5. Comparison of the observed (upper) and simulated (lower) spectra of the 0–0, $^sR_{21}$ branch, showing good agreement.

4. Validation of computed results

The output of this calculation generated by PGOPHER is provided in the form of a line list (online Supplement 2) consisting of the observed and calculated wavenumbers, Einstein A coefficients and f-values for 75 bands with $v=0$–8 in both electronic states. In order to validate the results we compared the observed spectra to those calculated by PGOPHER. The line shape of the calculated lines was changed by adjusting the Lorentzian and Gaussian contributions to the linewidths (Voigt line shape) in PGOPHER, in order to match it with the observed line shape. Next, the rotational temperature was estimated by varying it in small steps, and monitoring the intensity profile of a large number of rotational lines in the observed and simulated spectra. A value of ~720 K was estimated for the rotational temperature of this transition. In order to estimate the vibrational temperature, the rotational temperature was held fixed but the vibrational temperature was adjusted in steps. It was found that a vibrational temperature of the order of ~2000 K produced a simulated spectrum comparable to the observed spectrum. A portion of the spectrum of the 0–0 band near the Q_1 and R_1 heads of the $A^2\Pi_{3/2}$–$X^2\Sigma^+$, 0–0 band is presented in Fig. 3, comparing the simulated and the observed spectrum. As can be seen, a good correspondence exists. A portion of the observed spectrum of the $A^2\Pi_{1/2}$–$X^2\Sigma^+$, 1–0 band (upper plot) near the R_2 and $^sR_{21}$ heads has been compared with the simulated spectrum (lower plot) in Fig. 4, again showing a good agreement. Fig. 5 provides a portion of the $^sR_{21}$ branch of the 0–0 band, and compares the relative intensity of a few rotational lines in the observed (upper) and simulated (lower) spectra.

In general the two sub-bands of a $^2\Pi$–$^2\Sigma^+$ band have very similar intensity. In the case of the inverted $A^2\Pi$–$X^2\Sigma^+$ transition of CP, however, the higher energy $A^2\Pi_{1/2}$–$X^2\Sigma^+$ sub-band is about 35% weaker in intensity than the

$A^2\Pi_{3/2}$–$X^2\Sigma^+$ sub-band in our emission spectra. It seems likely that collisional relaxation between the two spin components of the $A^2\Pi$ state differs from the vibrational and rotational relaxation in our discharge tube and results in an anomalous relative population distribution between the different spin components.

In spite of extensive searches in different sources, CP has been observed only in the envelope of the carbon star IRC+10216, where other phosphorus bearing species such as PN and HCP have also been identified. This radical is mainly formed by photodissociation of HCP in the outer part of the shell. The intensity parameters of CP derived in the present work may prove useful in simulating the spectra of carbon stars.

5. Conclusion

The observed rotational line positions of the $A^2\Pi$–$X^2\Sigma^+$ bands, the derived spectroscopic constants for the $X^2\Sigma^+$, $A^2\Pi$ states and the electronic TDM of this transition obtained from high level *ab initio* calculations by de Brouckère and Feller [24] have been used to generate a line list containing transition wavenumbers, Einstein *A* coefficients and *f*-values for bands of this transition using the programs RKR1, LEVEL and PGOPHER. The TDM matrix elements calculated by LEVEL have been converted from Hund's case (b) to Hund's case (a) using a previously derived equation [29], so that the effect of spin angular momentum on the TDM matrix elements and the Herman–Wallis effect could be included. The line list is generated for 75 bands with $v=0$–8 for both the ground and excited electronic states. The number of *J* transitions reported are based on the highest observed *J* level for the vibrational levels of the band in question. This is explained in detail in the line list header. The radiative lifetimes of some lower vibrational levels of the $A^2\Pi$ state were computed using the Einstein *A* coefficients and compared with the theoretical values of Gu et al. [21]. The spectra of this transition were simulated with estimated rotational and vibrational temperatures and compared with observed spectra. The good agreement between the observed and simulated spectra validates the calculated line intensity parameters.

Acknowledgments

This research was supported by funding from the Leverhulme Trust of UK and the NASA laboratory astrophysics program. The spectra used in this work were recorded at the National Solar Observatory at Kitt Peak, AZ, USA.

Appendix A. Supplementary materials

Supplementary data associated with this article can be found in the online version at http://dx.doi.org/10.1016/j.jqsrt.2014.01.030.

References

[1] Guélin M, Cernicharo J, Paubert G, Turner BE. Free CP in IRC+10216. Astron Astrophys 1990;230:L9–11.
[2] Cernicharo J, Guélin M, Kahane C. A λ2 mm molecular line survey of the C-star envelope IRC+10216. Astron Astrophys Suppl 2000;142:181–215.
[3] Ziurys LM, Milam SN, Apponi AJ, Woolf NJ. Chemical complexity in the winds of the oxygen-rich supergiant star VY Canis Majoris. Nature 2007;447:1094–7.
[4] Tenenbaum ED, Woolf NJ, Ziurys LM. Identification of phosphorus monoxide ($X^2\Pi_r$) in VY Canis Majoris: detection of the first P–O bond in space. Astrophys J 2007;666:L29–32.
[5] Milam SN, Halfen DT, Tenenbaum ED, Apponi AJ, Woolf NJ, Ziurys LM. Constraining phosphorus chemistry in carbon- and oxygen-rich circumstellar envelopes: observations of PN, HCP, and CP. Astrophys J 2008;684:618–25.
[6] Herzberg G. A new band system probably due to a molecule CP. Nature (London) 1930;126:131–2.
[7] Bärwald H, Herzberg G, Herzberg L. Band spectra and structure of CP-molecules. Ann Phys (Leipzig) 1934;20:569–93.
[8] Chaudhury AK, Upadhya KN. $^2\Sigma^+$–$^2\Pi$ band system in CP molecule. Indian J Phys 1969;43:83–91.
[9] Tripathi R, Rai SB, Upadhya KN. The B-A system of CP molecule. Pramana 1981;17:249–55.
[10] Ram RS, Bernath PF. Fourier transform spectroscopy of the $A^2\Pi$–$X^2\Sigma^+$ system of CP. J Mol Spectrosc 1987;122:282–92.
[11] Saito S, Yamamoto S, Kawaguchi K, Ohishi M, Suzuki H, Ishikawa S, et al. The microwave spectrum of the CP radical and related astronomical search. Astrophys J 1989;341:1114–9.
[12] Klein H, Klisch E, Winnewisser G, Königshofen A, Hahn J. CP's triple-bond strength experienced in its THz spectrum. Z Naturforsch 1999;54a:187–90.
[13] Ram RS, Tam S, Bernath PF. The $A^2\Pi$–$X^2\Sigma^+$ system of CP: observation of new bands. J Mol Spectrosc 1992;152:89–100.
[14] Wentink T, Spindler RJ. Franck–Condon factors and r-centroids for NO^+, CP, SiF, BF, BCl, and BBr. J Quant Spectrosc Radiat Transf 1970;10:609–19.
[15] Murthy NS, Murthy BN. True potential energy curves for LaO, VO and CP. J Phys B 1970;3:Ll5–18.
[16] Murthy NS, Gowda LS, Murthy BN. Carbon phosphide ($B^2\Sigma^+$–$A^2\Pi_i$) band system: RKR Franck–Condon factors and *r*-centroids. Pramana 1976;6:25–8.
[17] Reddy RR, Rao TVR, Vishwanath R. Potential energy curves and dissociation energies of NbO, SiC, CP, PH^+, SiF^+ and NH^+. Astrophys Space Sci 1992;189:29–38.
[18] Shi DH, Xing X, Sun JF, Zhu ZL, Liu YF. Extensive *ab initio* study of the electronic states of CP radical including spin–orbit coupling. J Mol Spectrosc 2012;276–277:1–9.
[19] Rohlfing CM, Almlöf J. Theoretical determination of the dipole moment of carbon monophosphide, ($X^2\Sigma^+$). Chem Phys Lett 1988;147:258–62.
[20] de Brouckère G, Feller D. Configuration-interaction calculations of miscellaneous properties of the CP and CP^- molecules: I. CP ($X^2\Sigma^+$) ground state. J Phys B: At Mol Opt Phys 1996;29:5283–303.
[21] Gu J, Buenker RJ, Hirsch G. *Ab initio* CI study of the electronic spectrum of the interstellar free radical CP. Chem Phys 1994;185:39–45. (& Erratum: *Ab initio* CI study of the electronic spectrum of the interstellar free radical CP. Chem Phys 185 (1994) 39–45). 1994;188:107).
[22] McLean AD, Liu B, Chandler GS. Computed self-consistent field and singles and doubles configuration interaction spectroscopic data and dissociation energies for the diatomics B_2, C_2, N_2, O_2, F_2, CN, CP, CS, PN, SiC, SiN, SiO, SiP, and their ions. J Chem Phys 1992;97:8459–64.
[23] de Brouckère G. Configuration interaction calculations of miscellaneous properties of CP and CP^- molecules: II. CP^- ($X^1\Sigma^+$) ground state. J Phys B: At Mol Opt Phys 1997;30:1847–64.
[24] de Brouckère G, Feller D. Configuration interaction calculations on the $A^2\Pi_i$ state of CP and the $A^2\Pi_i$–$X^2\Sigma^+$ transition bands. Miscellaneous properties. J Phys B: At Mol Opt Phys 1998;31:5053–75.
[25] Le Roy RJ. Level 8.0: a computer program for solving the radial Schrödinger equation for bound and quasi-bound Levels. University of Waterloo Chemical Physics Research report. University of Waterloo; 2007.
[26] Western CM. PGOPHER, a program for simulating rotational structure (v.7.1.108); 2010. ⟨http://PGOPHER.chm.bris.ac.uk⟩.
[27] Li G, Harrison JJ, Ram RS, Western CW, Bernath PF. Einstein *A* coefficients and absolute line intensities for the $E^2\Pi$–$X^2\Sigma^+$ transition of CaH. J Quant Radiat Transf 2012;113:67–74.
[28] Brooke J, Bernath PF, Schmidt TW, Bacskay GB. Line strengths and updated molecular constants for the C_2 Swan system. J Quant Spectrosc Radiat Transf 2013;124:11–20.

[29] Brooke J, Ram RS, Western CM, Li G, Schwenke DW, Bernath PF. Einstein *A* coefficients and oscillator strengths for the $A^2\Pi$–$X^2\Sigma^+$ (red) and $B^2\Sigma^+$–$X^2\Sigma^+$ (violet) systems and rovibrational transitions in the $X^2\Sigma^+$ state of CN. Astrophys J Suppl Ser 2014;210:23(15pp).
[30] Bernath PF. Spectra of atoms and molecules. 2nd ed. Oxford University Press; 2005.
[31] Le Roy RJ. RKR1 2.0: a computer program implementing the first order RKR method for determining diatomic molecule potential energy functions. University of Waterloo Chemical Physics Research report. University of Waterloo; 2004.
[32] Herman R, Wallis RF. Influence of vibration–rotation interaction on line intensities in vibration–rotation bands of diatomic molecules. J Chem Phys 1955;23:637–46.
[33] Tipping RH, Bouanich J-P. On the use of Herman–Wallis factors for diatomic molecules. J Quant Spectrosc Radiat Transf 2001;71:99–103.